PHILOSOPHICAL TRANSACTIONS OF THE ROYAL SOCIETY A MATHEMATICAL, PHYSICAL & ENGINEERING SCIENCES

Symmetry Concepts for the Geometric Analysis of Mixing Flows

J. G. Franjione and J. M. Ottino

Phil. Trans. R. Soc. Lond. A 1992 **338**, 301-323
doi: 10.1098/rsta.1992.0010

Symmetry concepts for the geometric analysis of mixing flows

By J. G. Franjione[1] and J. M. Ottino[2]

[1]*Department of Chemical Engineering, University of Massachusetts, Amherst, Massachusetts 01003, U.S.A.*

[2]*Department of Chemical Engineering, Northwestern University, Evanston, Illinois 60208, U.S.A.*

Contents

Much of the recent analysis of chaotic mixing has focused on utilizing tools and techniques imported from dynamical systems theory. However, most techniques require detailed information about the velocity field or fluid motion and are restricted to conditions where the 'degree of chaos' is small. Symmetries provide a method of analysis without specific reference to exact mathematical expressions. Symmetry concepts are illustrated in terms of a prototypical system called the eggbeater flow. Although a family of 32 different eggbeater flows can be constructed, symmetry arguments reveal that only four of these are independent. These flows serve to illustrate the role of islands in mixing. If a flow possesses symmetry, islands are found in symmetric arrangements, the simplest cases being reflectional and rotational symmetries. A knowledge of symmetries provides the basis for systematic methods for destroying islands. These ideas are developed in terms of the eggbeater flows, and are subsequently extended to a class of three-dimensional continuous throughput flows – duct flows – which are of a more practical interest from an engineering viewpoint. Three such duct flows are studied. Using symmetries, we show that these flows are topologically identical to the eggbeater flows, even though their geometries and flow mechanisms are quite different from the eggbeater flows. Lastly, we demonstrate how the same methodology for destroying islands and enhancing mixing in the eggbeater flows can be applied to duct flows.

Phil. Trans. R. Soc. Lond. A (1992) **338**, 301–323
Printed in Great Britain

1. Introduction

Fluid mixing is an important operation which occurs in a variety of scientific and engineering applications. In general, mixing occurs via three distinct mechanisms: mechanical mixing (stretching and folding of fluid elements), breakup, and molecular diffusion; often processes are accompanied by chemical reaction as well (Ottino 1989*a*). However, mechanical mixing is the one mechanism over which the greatest control is possessed, and hence improving mechanical mixing provides the best means for enhancing mixing processes in which all mechanisms are present.

The goal of mechanical mixing (henceforth referred to simply as mixing) is to create a maximum amount of intermaterial area while consuming the least energy possible in a given amount of time. On one level, then, the study of mixing reduces to understanding how, why, and what types of flows are capable of efficient stretching. A possible way to attack this question is in terms of dynamical systems. Indeed, such an approach has proved fruitful. During the past few years it has been established, by analysis, computation, and experiment, that all flows which exhibit characteristics of good mixing must also exhibit the characteristics of chaos.

The formulation of a systematic mathematical theory for the analysis of chaotic mixing, however, remains to be developed (for a review of these issues see Aref (1990) and Ottino (1989*a*)). Isolated mathematical treatments are available from the mathematics and physics literature, but no general methods of attack have been proposed. Most theory applies to systems characterized by small perturbations from integrability. However, in many cases involving mixing flows, there is no sensible integrable picture to speak of. Additionally, although small perturbation techniques, such as the Melnikov method and adiabatic invariants, provide valuable insight, they implicitly address cases in which mixing is poor (i.e. when good mixing is restricted to small regions of the flow or stochastic layers). Finally, most analytical techniques require detailed information about either the fluid motion or the velocity field. It is desirable to seek methods that are independent of the details of flow fields.

In this paper we present a few ideas, inspired by geometrical arguments, that attempt to remedy this situation. An analysis of symmetries accomplishes this objective. Symmetries exist whenever there are simple geometric constraints on the fluid motion; e.g. system geometry, flow conditions, etc. Techniques can be developed to analyse time-periodic and spatially periodic flows; an important advantage of these techniques is that the analysis is not restricted to small perturbations.

We have already shown in a previous paper how symmetries can be exploited to enhance mixing, and demonstrated their use in terms of an experimental example (Franjione *et al.* 1989). In this work, we put the discussion into a more general framework, and show how to apply symmetries to a wide class of problems. The presentation is intended to serve as a self-contained source for the subject, so that the interested reader can learn all the details without reference outside sources. We begin with an analysis of two-dimensional flows, in terms of a simple class of prototype flows, called the *eggbeater flow family*. These flows provide a setting for a discussion of how to find symmetries and how they can be exploited to enhance mixing. This analysis then serves as a springboard for the analysis of systems which are of a more practical interest from an engineering standpoint: three-dimensional continuous throughput flows, which we refer to as *duct flows*. Lastly, we discuss how the same

PHILOSOPHICAL TRANSACTIONS OF THE ROYAL SOCIETY A MATHEMATICAL, PHYSICAL & ENGINEERING SCIENCES

techniques used to enhance mixing in the two-dimensional flows can be applied to the duct flows.

2. Mixing in two dimensions: the eggbeater flow

Mixing is necessarily poor in all steady two-dimensional flows. A two-dimensional steady flow can be completely characterized by a time-invariant streamline portrait; streamlines coincide with pathlines, and fluid elements are constrained to lie within the same streamlines for all time. Thus fluid elements can never be distributed homogeneously throughout the flow domain.

Let us now define some terminology to provide a setting for the rest of the discussion. We refer to the mechanism by which material is deformed in space along the streamlines in a two-dimensional steady flow as *stretching*. Any flow which consists of stretching alone is a poor mixing flow. To improve mixing, material must somehow be released from the constraint of being bounded by the same streamlines for all time. This can be accomplished by altering the orientation of the streamline portrait with respect to the placement of the material (or vice versa). We call this mechanism *reorientation*. The only way to achieve reorientation in a two-dimensional flow is by periodically changing the shape of the streamlines, which we refer to as *streamline modulation*. (Such an effect, for example, can be achieved by changing the topology of the streamline portrait.) Such a modulation can be achieved by various means. One possibility is to modulate the flow via boundary conditions such as out-of-phase motion of boundaries in Stokes flows; another possibility is to exploit the natural oscillations in flow due an increase in Reynolds or Rayleigh number as in the case of the Taylor–Couette flow or the Rayleigh–Bénard flow. The sequence of actions changing the streamline sequence is referred to as the *mixing protocol* or *flow sequence*. If the superposition of two streamline portraits taken at arbitrary times produces crossings, then the constraint of confining streamlines disappears. If the protocol is time-periodic, the crossings can create a special type of folding called a horseshoe map, which is one of the signatures of a chaotic dynamical system. Stretching accompanied by this type of folding results in effective mixing (Ottino 1989*a*).

The mixing, however, need not be widespread. It is possible for completely segregated poorly mixed regions to exist in the flow simultaneously with well-mixed chaotic regions. These regions are called *islands*. Fluid inside an island can never escape, and fluid outside an island can never enter. Islands are not stagnant regions, but in fact translate and rotate during flow. The simplest picture is revealed when the system is examined at suitable times; in such cases the placement of the islands become symmetric and the analysis of the system is simplified considerably.

Symmetries provide clues as to how to improve mixing and the focus here is on the best way of combining periodic protocols to accomplish this objective. Poincaré sections offer useful guidance in this regard. A Poincaré section is, in a very real sense, a 'phase plane' of a mapping, in the same manner that a plot of $\mathrm{d}\boldsymbol{x}/\mathrm{d}t = \boldsymbol{v}(\boldsymbol{x})$ is the phase plane of the ODE system. Such a plot gives an asymptotic picture of the behaviour for long times indicating regions of 'good' and 'poor' mixing (islands). Although the details of this picture will depend on the period of the mixing protocol, as of now, they cannot be obtained from the equations themselves without recourse to computation. The goal of constructing an efficient flow sequence is to enable all material in the flow to be found, at least for some significant fraction of the time, in regions of good mixing.

These concepts can be illustrated in terms of a simple example which we develop throughout the rest of the paper. Consider a unidirectional flow of the form:

$$\mathrm{d}x/\mathrm{d}t = v(y), \quad \mathrm{d}y/\mathrm{d}t = 0.$$

These equations can easily be integrated to yield the motion:

$$x = X + v(Y)t, \quad y = Y.$$

The velocity profile $v(\xi)$ is still unspecified. However, no matter what the form of $v(\xi)$, the mixing is poor since material tends to become aligned with the x-axis. To enhance stretching, we simply rotate the system by 90°, so that material which was originally aligned parallel with the streamlines is now oriented normal to the streamlines. We refer to this sequence of orthogonally oriented flows as the *eggbeater flow* (EBF), since it represents a simplified picture of the mixing mechanism in a hand-held eggbeater (Ottino 1989*b*). In order to eliminate loss of material, we assume that the flow occurs in a domain which is periodic in both the x and y directions. The domain of the flow is given by $-1 \leqslant x \leqslant 1$ and $-1 \leqslant y \leqslant 1$. When a particle exits through one side of the box, it reenters the box at the opposite side. Using the physical model of the eggbeater, this can be interpreted to be that whenever a blade leaves the domain, a new blade enters on the opposite side. In geometrical terms, the flow occurs on a torus.

The overall flow may be expressed as a mapping, composed of two different parts. The first flow acts in a horizontal direction:

$$x_{n+1} = x_n + Tv(y_n), \quad y_{n+1} = y_n,$$

where T is the amount of time that the first flow acts, i.e. the length of time the rod is dragged in the x-direction. We denote this flow as $\boldsymbol{H}$, and we write the flow as $\boldsymbol{x}_{n+1} = \boldsymbol{H}\boldsymbol{x}_n$, where $\boldsymbol{x} = (x, y)$. The second flow acts in a vertical direction for time T also:

$$x_{n+1} = x_n, \quad y_{n+1} = y_n + Tv(x_n)$$

and we write this flow as $x_{n+1} = \boldsymbol{V}\boldsymbol{x}_n$. The overall mapping may be written as the composition of both maps, i.e.:

$$\boldsymbol{x}_{n+1} = \boldsymbol{V}\boldsymbol{H}\boldsymbol{x}_n = \boldsymbol{E}\boldsymbol{x}_n.$$

A sequence of actions of the horizontal and vertical components, $\boldsymbol{H}$ and $\boldsymbol{V}$, is denoted as $\boldsymbol{VHVHVH}$, and is an example of a *mixing protocol*.

3. Algebra of symmetries

As a first step toward understanding the EBF, we first investigate the basic geometrical properties of the motion. The first object is to exploit any algebraic relationships which exist between $\boldsymbol{V}$ and $\boldsymbol{H}$. Note that the vertical flow can be expressed in terms of the horizontal flow. The flow $\boldsymbol{V}$ can be equivalently realized by first rotating the entire domain by $-90°$ about the origin, running the $\boldsymbol{H}$ flow, and then rotating back by 90° (see figure 1). We write this as

$$\boldsymbol{V} = \boldsymbol{R}\boldsymbol{H}\boldsymbol{R}^{-1},$$

where $\boldsymbol{R}$ represents rotations by 90°; i.e. $(x, y) \rightarrow (-y, x)$. The EBF may be written as

$$\boldsymbol{x}_{n+1} = \boldsymbol{R}\boldsymbol{H}\boldsymbol{R}^{-1}\boldsymbol{H}\boldsymbol{x}_n.$$

Figure 1

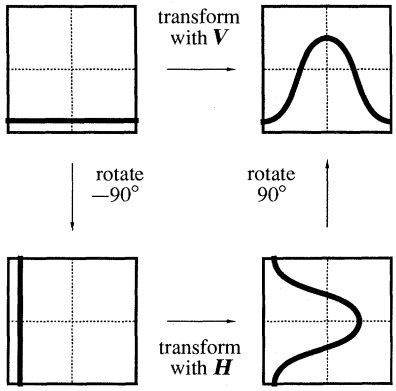

Figure 2

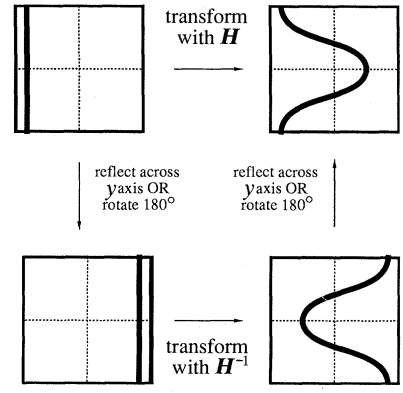

Figure 1. Relationship between $\boldsymbol{H}$ and $\boldsymbol{V}$. A deformation due to the vertical flow is equivalent to first rotating the domain by $-90°$, operating with the horizontal flow, and then rotating back by 90°. Note that although the velocity profile shown is even about the origin, the validity of the relationship does not depend on this.

Figure 2. Symmetries between $\boldsymbol{H}$ and $\boldsymbol{H}^{-1}$ when the velocity profile is even about the origin. Symmetry with respect to reflections across the y-axis is shown by noting that motion due to $\boldsymbol{H}$ can be accomplished by first reflecting across the y-axis, transforming with $\boldsymbol{H}^{-1}$, and then reflecting back across the y-axis. $\boldsymbol{H}$ is also symmetric to its inverse with respect to 180° rotations.

Deduction of other relationships is facilitated through the introduction of the concept of symmetry.

There exist many definitions for symmetries, depending on the application (Golubitsky *et al.* 1985; Chossat & Golubitsky 1988; de Vogalaere 1958; Greene *et al.* 1981). Here, we introduce a definition of symmetry suitable to our needs. We say that two flows, $\boldsymbol{A}$ and $\boldsymbol{B}$, are symmetric to each other if a transformation $\boldsymbol{S}$ can be found such that:

$$\boldsymbol{B} = \boldsymbol{S}\boldsymbol{A}\boldsymbol{S}^{-1}.$$

We consider two types of symmetries: *ordinary* symmetry, when both $\boldsymbol{A}$ and $\boldsymbol{B}$ are the same (in which a flow itself possesses a certain symmetry) and *time-reversal* symmetry in which $\boldsymbol{B}$ is the inverse of $\boldsymbol{A}$, i.e. $\boldsymbol{B} = \boldsymbol{S}\boldsymbol{B}^{-1}\boldsymbol{S}^{-1}$. (This definition is more general than the one used in Franjione *et al.* (1989), as we extend the definition to allow ordinary symmetry.)

There exist generalized algorithms for finding the symmetries of mappings (Olver 1986); however, it is often simpler to use geometric intuition. The first task is to find simple relationships involving the individual elements which compose the map in question, and then use these relations to find some of the symmetries. For the EBF, this involves finding relationships for $\boldsymbol{H}$, the horizontal shear flow.

When the velocity profile $v(\xi)$ is even about the origin, $\boldsymbol{H}$ is symmetric to its inverse with respect to reflections across the y-axis, and also with respect to 180° rotations about the origin (see figure 2). Additionally, $\boldsymbol{H}$ is symmetric to itself about reflections across the x-axis. Symbolically, we represent these relationships as:

$$\boldsymbol{H} = \boldsymbol{S}_y\boldsymbol{H}^{-1}\boldsymbol{S}_y, \quad \boldsymbol{H} = \boldsymbol{R}^2\boldsymbol{H}^{-1}\boldsymbol{R}^2, \quad \boldsymbol{H} = \boldsymbol{S}_x\boldsymbol{H}\boldsymbol{S}_x,$$

where $\boldsymbol{S}_x = (x, y) \to (x, -y)$, i.e. reflection across the x-axis, $\boldsymbol{S}_y = (x, y) \to (-x, y)$, reflection across the y-axis, and $\boldsymbol{R}^2 = (x, y) \to (-x, -y)$, i.e. 90° rotations. Symmetry

can also be interpreted in terms of particle trajectories. Consider, for example, the $\boldsymbol{R}^2$ symmetry of $\boldsymbol{H}$. If the flow carries a particle from $\boldsymbol{a}$ to $\boldsymbol{b}$, the same motion can be accomplished by first rotating by 180° to $\boldsymbol{a}'$, running the inverse flow, which takes the particle to $\boldsymbol{b}'$, and then rotating by 180° back to $\boldsymbol{b}$.

Transformations are either orientation preserving or orientation reversing. The character of a two-dimensional map $\boldsymbol{M}$ is determined by its jacobian matrix, $\boldsymbol{J}_M$, calculated as:

$$\boldsymbol{J}_M = (\partial x_{n+1}, \partial y_{n+1})/(\partial x_n, \partial y_n).$$

If the determinant of $\boldsymbol{J}_M$ is -1, the transformation is orientation reversing, and if the determinant is $+1$, the transformation is orientation preserving. If the transformation is a symmetry, then other distinctions are made. A symmetry which is orientation preserving (such as $\boldsymbol{R}^2$, one of the time-reversal symmetries of $\boldsymbol{H}$), is called a *rotational* symmetry, or rotation, and a symmetry which is orientation reversing (such as $\boldsymbol{S}_x$ or $\boldsymbol{S}_y$) is called a *reflectional* symmetry, or reflection.

It can be shown that the eggbeater flow can be written as the second iterate of a different map. Recall that above we wrote the EBF as

$$\boldsymbol{E} = \boldsymbol{RHR}^{-1}\boldsymbol{H}. \tag{1}$$

However, $\boldsymbol{H}$ is symmetric about the x-axis; i.e. $\boldsymbol{H} = \boldsymbol{S}_x \boldsymbol{H} \boldsymbol{S}_x$. Substituting into equation (1) above, we obtain

$$\boldsymbol{E} = \boldsymbol{RS}_x \boldsymbol{HS}_x \boldsymbol{R}^{-1}\boldsymbol{H}.$$

The rotation operator $\boldsymbol{R}$ is symmetric to its inverse with respect to reflections across the x-axis. Therefore, we have $\boldsymbol{R} = \boldsymbol{S}_x \boldsymbol{R}^{-1} \boldsymbol{S}_x$, or equivalently, $\boldsymbol{RS}_x = \boldsymbol{S}_x \boldsymbol{R}^{-1}$. Letting $\boldsymbol{S}_1 = \boldsymbol{RS}_x$, which is given by $\boldsymbol{S}_1 : (x, y) \to (y, x)$, i.e. reflection about the 45° line. This $\boldsymbol{E}$ can be expressed as

$$\boldsymbol{E} = \boldsymbol{S}_1 \boldsymbol{H} \boldsymbol{S}_1 \boldsymbol{H} = (\boldsymbol{S}_1 \boldsymbol{H})^2.$$

Thus the eggbeater map $\boldsymbol{E}$ is actually the second iterate of a second map, $\boldsymbol{S}_1 \boldsymbol{H} = \boldsymbol{E}_{\mathrm{f}}$, which we refer to as the *fundamental* eggbeater map. However, although $\boldsymbol{E}$ itself is an orientation preserving transformation, it is interesting to note that since $\det \boldsymbol{J}_H = 1$, and $\det \boldsymbol{J}_{S1} = -1$, then $\det \boldsymbol{J}_{E\mathrm{f}} = -1$, and so the fundamental eggbeater map is orientation reversing. In fact, we shall encounter another example of this type of map in §7, when we investigate duct flows.

4. Generalized eggbeater flows

The expression of the eggbeater flow $\boldsymbol{E} = \boldsymbol{VH}$ as $\mathrm{E} = \boldsymbol{RHR}^{-1}\boldsymbol{H}$ suggests the introduction of a family of 'generalized eggbeater flow', in which the directions (forward or inverse) of $\boldsymbol{R}$ and $\boldsymbol{H}$, and the 'evenness' or 'oddness' of the velocity profile are unspecified:

$$\begin{aligned} \boldsymbol{x}_{n+1} &= \boldsymbol{R}^{2d-1} \boldsymbol{H}_k^{2c-1} \boldsymbol{R}^{2b-1} \boldsymbol{H}_k^{2a-1} \boldsymbol{x}_n \\ &= \boldsymbol{E}_{k,dbca}\, \boldsymbol{x}_n. \end{aligned}$$

The subscripts a, b, c and d can be set to 0 or 1 and the set of values is denoted as $\{\ldots\}$. Note that when any of $\{a, b, c, d\}$ is set to 1, the exponent equals 1 (forward motion, in the direction $x > 0$, $y > 0$, or counterclockwise rotation), and when any $\{a, b, c, d\}$ is 0, the exponent equals -1 (backward motion, direction $x < 0$, $y < 0$, or clockwise

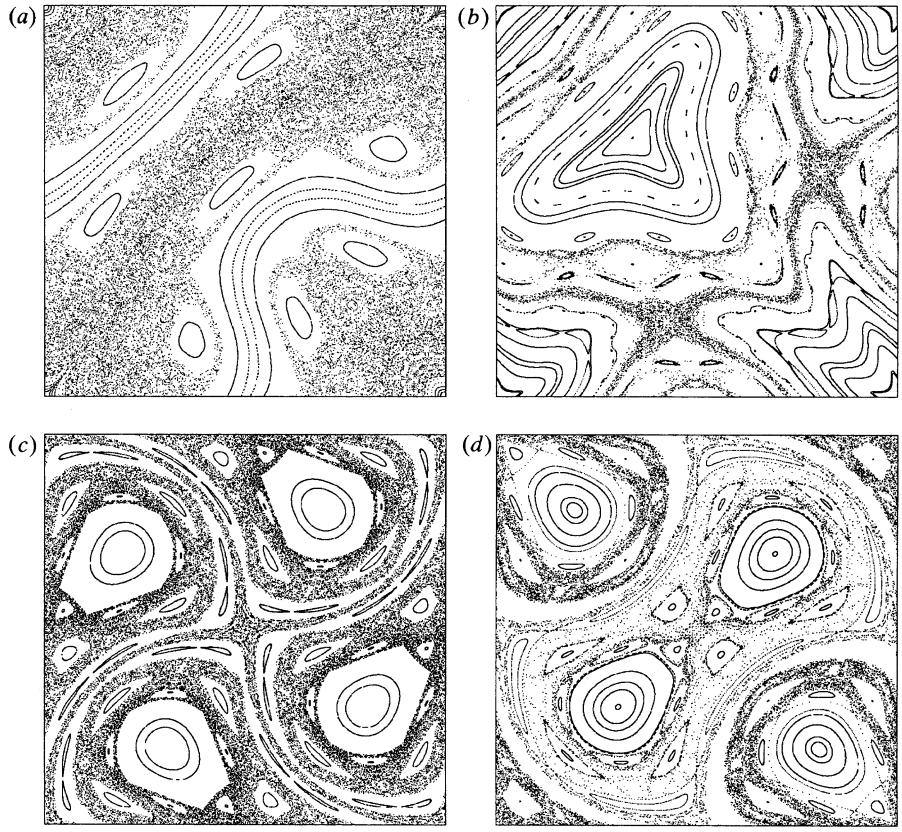

Figure 3. Representative Poincaré sections of the fundamental eggbeater flows (all correspond to $T = 0.4$). (*a*) $\boldsymbol{E}_{\mathrm{Re}}$ (even velocity profile, orientation reversing mapping); (*b*) $\boldsymbol{E}_{\mathrm{Pe}}$ (even velocity profile, orientation preserving mapping); (*c*) $\boldsymbol{E}_{\mathrm{Ro}}$ (odd velocity profile with maximum value at 0.25, orientation reversing mapping); (*d*) $\boldsymbol{E}_{\mathrm{Po}}$ (odd velocity profile with maximum value at 0.25, orientation preserving mapping).

rotation). We allow k to be 'e' or 'o', indicating evenness or oddness of $v(\xi)$ about the origin. In this notation, the eggbeater flow $\boldsymbol{VH}$ above, with $v(\xi)$ even, would be referred to as $\boldsymbol{E}_{\mathrm{e},1101}$. From this formulation, 32 different eggbeater flows can be constructed. However, it can be shown that only 4 of the flows are independent. For $v(\xi)$ even, the flows are $\boldsymbol{E}_{\mathrm{e},1101}$ and $\boldsymbol{E}_{\mathrm{e},1111}$; for $v(\xi)$ odd, they are $\boldsymbol{E}_{\mathrm{o},1001}$ and $\boldsymbol{E}_{\mathrm{o},1111}$. We refer to these four flows as $\boldsymbol{E}_{\mathrm{Re}}, \boldsymbol{E}_{\mathrm{Pe}}, \boldsymbol{E}_{\mathrm{Ro}}$ and $\boldsymbol{E}_{\mathrm{Po}}$:

$$\boldsymbol{E}_{\mathrm{Re}} = \boldsymbol{R}\boldsymbol{H}_{\mathrm{e}}\boldsymbol{R}^{-1}\boldsymbol{H}_{\mathrm{e}},$$

$$\boldsymbol{E}_{\mathrm{Pe}} = \boldsymbol{R}\boldsymbol{H}_{\mathrm{e}}\boldsymbol{R}\boldsymbol{H}_{\mathrm{e}},$$

$$\boldsymbol{E}_{\mathrm{Ro}} = \boldsymbol{R}\boldsymbol{H}_{\mathrm{o}}^{-1}\boldsymbol{R}^{-1}\boldsymbol{H}_{\mathrm{o}},$$

$$\boldsymbol{E}_{\mathrm{Po}} = \boldsymbol{R}\boldsymbol{H}_{\mathrm{o}}\boldsymbol{R}\boldsymbol{H}_{\mathrm{o}}.$$

(The 'P' and 'R' subscripts denote whether the corresponding fundamental mapping is orientation preserving or reversing. This aspect shall be explored in greater detail later in this section.) Some representative Poincaré sections are shown in figure 3. For these plots, we use

$$v(\xi) = 2[V_s + (1 - V_s)(1 - \xi^2)^2]$$

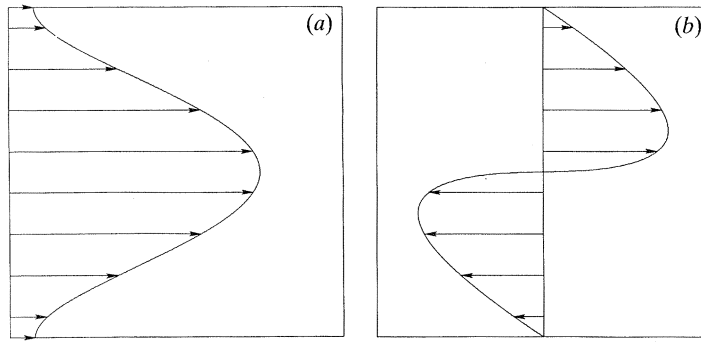

Figure 4. Velocity profiles used for computational investigations of eggbeater flow. (*a*) $v(\xi)$ even; (*b*) $v(\xi)$ odd.

Table 1. (*a*) *Equivalence of eggbeater flows with an even velocity profile. All flows are equivalent to either* $\boldsymbol{E}_{\mathrm{Pe}}$ *or* $\boldsymbol{E}_{\mathrm{Re}}$. (*b*) *Equivalence of eggbeater flows with an odd velocity profile. All flows are equivalent to either* $\boldsymbol{E}_{\mathrm{Po}}$ *or* $\boldsymbol{E}_{\mathrm{Ro}}$.

(*a*)	*d*	*b*	*c*	*a*	equiv. to	rel. by	(*b*)	*d*	*b*	*c*	*a*	equiv. to	rel. by
1	1	1	1	1	$\boldsymbol{E}_{\mathrm{Pe}}$	—	1	1	1	1	1	$\boldsymbol{E}_{\mathrm{Po}}$	—
2	1	1	0	1	$\boldsymbol{E}_{\mathrm{Re}}$	—	2	1	1	0	1	$\boldsymbol{E}_{\mathrm{Po}}$	—
3	0	1	1	1	$\boldsymbol{E}_{\mathrm{Re}}$	$\boldsymbol{S}_x$	3	0	1	1	1	$\boldsymbol{E}_{\mathrm{Po}}$	—
4	0	1	0	1	$\boldsymbol{E}_{\mathrm{Pe}}$	$\boldsymbol{S}_x$	4	0	1	0	1	$\boldsymbol{E}_{\mathrm{Po}}$	—
5	1	0	1	0	$\boldsymbol{E}_{\mathrm{Pe}}$	$\boldsymbol{R}^2$	5	1	0	1	0	$\boldsymbol{E}_{\mathrm{Po}}$	$\boldsymbol{S}_{x,y}$
6	1	0	0	0	$\boldsymbol{E}_{\mathrm{Re}}$	$\boldsymbol{R}^2$	6	1	0	0	0	$\boldsymbol{E}_{\mathrm{Po}}$	$\boldsymbol{S}_{x,y}$
7	0	0	1	0	$\boldsymbol{E}_{\mathrm{Re}}$	$\boldsymbol{S}_y$	7	0	0	1	0	$\boldsymbol{E}_{\mathrm{Po}}$	$\boldsymbol{S}_{x,y}$
8	0	0	0	0	$\boldsymbol{E}_{\mathrm{Pe}}$	$\boldsymbol{S}_y$	8	0	0	0	0	$\boldsymbol{E}_{\mathrm{Po}}$	$\boldsymbol{S}_{x,y}$
9	1	0	1	1	$\boldsymbol{E}_{\mathrm{Pe}}$	$\boldsymbol{S}_x$	9	1	0	1	1	$\boldsymbol{E}_{\mathrm{Ro}}$	—
10	1	0	0	1	$\boldsymbol{E}_{\mathrm{Re}}$	$\boldsymbol{S}_x$	10	1	0	0	1	$\boldsymbol{E}_{\mathrm{Ro}}$	—
11	0	0	1	1	$\boldsymbol{E}_{\mathrm{Re}}$	—	11	0	0	1	1	$\boldsymbol{E}_{\mathrm{Ro}}$	—
12	0	0	0	1	$\boldsymbol{E}_{\mathrm{Pe}}$	—	12	0	0	0	1	$\boldsymbol{E}_{\mathrm{Ro}}$	—
13	1	1	1	0	$\boldsymbol{E}_{\mathrm{Pe}}$	$\boldsymbol{S}_y$	13	1	1	1	0	$\boldsymbol{E}_{\mathrm{Ro}}$	$\boldsymbol{S}_{x,y}$
14	1	1	0	0	$\boldsymbol{E}_{\mathrm{Re}}$	$\boldsymbol{S}_y$	14	1	1	0	0	$\boldsymbol{E}_{\mathrm{Ro}}$	$\boldsymbol{S}_{x,y}$
15	0	1	1	0	$\boldsymbol{E}_{\mathrm{Re}}$	$\boldsymbol{R}^2$	15	0	1	1	0	$\boldsymbol{E}_{\mathrm{Ro}}$	$\boldsymbol{S}_{x,y}$
16	0	1	0	0	$\boldsymbol{E}_{\mathrm{Pe}}$	$\boldsymbol{R}^2$	16	0	1	0	0	$\boldsymbol{E}_{\mathrm{Ro}}$	$\boldsymbol{S}_{x,y}$

for the velocity profile which is even about the origin and

$$v(\xi) = -4(1-|\xi|^{\alpha})|\xi|^{\alpha} \quad \text{for} \quad -1 \leqslant \xi \leqslant 0,$$

$$= 4(1-\xi^{\alpha})\,\xi^{\alpha} \qquad \text{for} \quad 0 \leqslant \xi \leqslant 1,$$

where $\alpha = -\ln 2/\ln \xi_{\max}$ for the velocity profile which is odd about the origin. In the first profile, V_s is the 'slip velocity', i.e. the velocity of particles located on the domain boundary. In the second, $\pm\xi_{\max}$ is the location of the maximum/minimum in the velocity profile. The two profiles are shown in figure 4.

The equivalence of each of the 32 different eggbeater flows to $\boldsymbol{E}_{\mathrm{Re}}$, $\boldsymbol{E}_{\mathrm{Pe}}$, $\boldsymbol{E}_{\mathrm{Ro}}$ or $\boldsymbol{E}_{\mathrm{Po}}$ is shown in table 1. For example, consider the flow $\boldsymbol{E}_{\mathrm{e},0111} = \boldsymbol{R}^{-1}\boldsymbol{H}_{\mathrm{e}}\boldsymbol{R}\boldsymbol{H}_{\mathrm{e}}$. The rotation operator, $\boldsymbol{R}$, is symmetric to its inverse with respect to reflections across the x-axis, i.e.:

$$\boldsymbol{R} = \boldsymbol{S}_x\boldsymbol{R}^{-1}\boldsymbol{S}_x.$$

PHILOSOPHICAL TRANSACTIONS OF THE ROYAL SOCIETY A MATHEMATICAL, PHYSICAL & ENGINEERING SCIENCES

Substituting this relation into the above expression for $\boldsymbol{E}_{\mathrm{e},0111}$, we obtain:

$$\boldsymbol{E}_{\mathrm{e},0111} = \boldsymbol{S}_x \boldsymbol{R} \boldsymbol{S}_x \boldsymbol{H}_{\mathrm{e}} \boldsymbol{S}_x \boldsymbol{R}^{-1} \boldsymbol{S}_x \boldsymbol{H}_{\mathrm{e}}.$$

However, since $\boldsymbol{H}_{\mathrm{e}}$ is an even function about the origin, then $\boldsymbol{H}_{\mathrm{e}} = \boldsymbol{S}_x \boldsymbol{H}_{\mathrm{e}} \boldsymbol{S}_x$ (or $\boldsymbol{S}_x \boldsymbol{H}_{\mathrm{e}} = \boldsymbol{H}_{\mathrm{e}} \boldsymbol{S}_x$), this expression can be rearranged to give:

$$\begin{aligned} \boldsymbol{E}_{\mathrm{e},0111} &= \boldsymbol{S}_x [\boldsymbol{R} \boldsymbol{H}_{\mathrm{e}} \boldsymbol{R}^{-1} \boldsymbol{H}_{\mathrm{e}}] \boldsymbol{S}_x \\ &= \boldsymbol{S}_x \boldsymbol{E}_{\mathrm{e},1101} \boldsymbol{S}_x = \boldsymbol{S}_x \boldsymbol{E}_{\mathrm{Re}} \boldsymbol{S}_x. \end{aligned}$$

When $v(\xi)$ is odd, $\boldsymbol{H}_{\mathrm{o}}$ is symmetric to its inverse with respect to reflections across the x- and y-axes, and is itself symmetric with respect to 180° rotations about the origin. This is expressed as:

$$\boldsymbol{H}_{\mathrm{o}} = \boldsymbol{S}_y \boldsymbol{H}_{\mathrm{o}}^{-1} \boldsymbol{S}_y, \quad \boldsymbol{H}_{\mathrm{o}} = \boldsymbol{S}_x \boldsymbol{H}_{\mathrm{o}}^{-1} \boldsymbol{S}_x, \quad \boldsymbol{H}_{\mathrm{o}} = \boldsymbol{R}^2 \boldsymbol{H}_{\mathrm{o}} \boldsymbol{R}^2.$$

These relationships are necessary for showing equivalence among the odd flows.

Obviously, $\boldsymbol{E}_{\mathrm{Pe}}$ and $\boldsymbol{E}_{\mathrm{Po}}$ are the second iterates of the maps $\boldsymbol{R}\boldsymbol{H}_{\mathrm{e}}$ and $\boldsymbol{R}\boldsymbol{H}_{\mathrm{o}}$ respectively. We have already shown how $\boldsymbol{E}_{\mathrm{Re}}$ is the second iterate of the map $\boldsymbol{S}_1 \boldsymbol{H}_{\mathrm{e}}$. Similarly, it can be shown that $\boldsymbol{E}_{\mathrm{Ro}}$ is the second iterate of the orientation reversing map $\boldsymbol{S}_1 \boldsymbol{H}_{\mathrm{o}}$.

The four 'fundamental' maps are:

$$\boldsymbol{E}_{\mathrm{fRe}} = \boldsymbol{S}_1 \boldsymbol{H}_{\mathrm{e}}, \tag{2}$$

$$\boldsymbol{E}_{\mathrm{fPe}} = \boldsymbol{R}\boldsymbol{H}_{\mathrm{e}}, \tag{3}$$

$$\boldsymbol{E}_{\mathrm{fRo}} = \boldsymbol{S}_1 \boldsymbol{H}_{\mathrm{o}}, \tag{4}$$

$$\boldsymbol{E}_{\mathrm{fPo}} = \boldsymbol{R}\boldsymbol{H}_{\mathrm{o}}, \tag{5}$$

Earlier, we utilized symmetry properties of the individual components of the EBFS to find these fundamental mappings. Now we focus on finding the symmetries of the fundamental mappings themselves. We analyse the first and fourth flows in detail.

Recall that $\boldsymbol{H}_{\mathrm{e}}$ is symmetric to its inverse with respect to 180° rotations about the origin. Substituting this relationship into equation (2), we have

$$\boldsymbol{E}_{\mathrm{fRe}} = \boldsymbol{S}_1 \boldsymbol{R}^2 \boldsymbol{H}_{\mathrm{e}}^{-1} \boldsymbol{R}^2.$$

Inserting the identity operator, in the form of $\boldsymbol{S}_1 \boldsymbol{S}_1$, we have

$$\boldsymbol{E}_{\mathrm{fRe}} = \boldsymbol{S}_1 \boldsymbol{R}^2 [\boldsymbol{H}_{\mathrm{e}}^{-1} \boldsymbol{S}_1] \boldsymbol{S}_1 \boldsymbol{R}^2.$$

However, the term enclosed in the square brackets is simply the inverse of the initial map. Letting $\boldsymbol{S}_1 \boldsymbol{R}^2 = \boldsymbol{S}_2$, i.e. the transformation $(x, y) \rightarrow (-y, -x)$, reflections about the $-45°$ line, we obtain the relationship

$$\boldsymbol{E}_{\mathrm{fRe}} = \boldsymbol{S}_2 \boldsymbol{E}_{\mathrm{fRe}}^{-1} \boldsymbol{S}_2$$

indicating that $\boldsymbol{E}_{\mathrm{fRe}}$ is symmetric to its inverse with respect to reflections across the $-45°$ line.

To analyse $\boldsymbol{E}_{\mathrm{fPo}}$, we first make use of the fact that $\boldsymbol{H}_{\mathrm{o}}$ is symmetric to its inverse with respect to reflections about either the x- or y-axis. We write this as

$$\boldsymbol{H}_{\mathrm{o}} = \boldsymbol{S}_{x,y} \boldsymbol{H}_{\mathrm{o}}^{-1} \boldsymbol{S}_{x,y}.$$

Therefore, $\boldsymbol{E}_{\mathrm{fPo}}$ can be expressed as

$$\boldsymbol{E}_{\mathrm{fPo}} = \boldsymbol{R} \boldsymbol{S}_{x,y} \boldsymbol{H}_{\mathrm{o}}^{-1} \boldsymbol{S}_{x,y}.$$

Table 2. *Symmetries of the independent eggbeater flows* $\boldsymbol{E}_{\mathrm{Pe}}$, $\boldsymbol{E}_{\mathrm{Re}}$, $\boldsymbol{E}_{\mathrm{Po}}$ *and* $\boldsymbol{E}_{\mathrm{Ro}}$.

flow	full mapping	fundamental mapping	time-reversal symmetries	ordinary symmetries
$\boldsymbol{E}_{\mathrm{Pe}}$	$\boldsymbol{R}\boldsymbol{H}_{\mathrm{e}}\boldsymbol{R}\boldsymbol{H}_{\mathrm{e}}$	$\boldsymbol{R}\boldsymbol{H}_{\mathrm{e}}$	$-45°$ line	none
$\boldsymbol{E}_{\mathrm{Re}}$	$\boldsymbol{R}\boldsymbol{H}_{\mathrm{e}}\boldsymbol{R}^{-1}\boldsymbol{H}_{\mathrm{e}}$	$\boldsymbol{S}_1\boldsymbol{H}_{\mathrm{e}}$	$-45°$ line	none
$\boldsymbol{E}_{\mathrm{Po}}$	$\boldsymbol{R}\boldsymbol{H}_{\mathrm{o}}\boldsymbol{R}\boldsymbol{H}_{\mathrm{o}}$	$\boldsymbol{R}\boldsymbol{H}_{\mathrm{o}}$	$\pm 45°$ lines	$180°$ rotations
$\boldsymbol{E}_{\mathrm{Ro}}$	$\boldsymbol{R}\boldsymbol{H}_{\mathrm{o}}^{-1}\boldsymbol{R}^{-1}\boldsymbol{H}_{\mathrm{o}}$	$\boldsymbol{S}_{1,2}\boldsymbol{H}_{\mathrm{o}}$	$\pm 90°$ rotations	$180°$ rotations

Inserting the identity operator, as $\boldsymbol{R}^{-1}\boldsymbol{R}$, we have

$$\boldsymbol{E}_{\mathrm{fPo}} = \boldsymbol{R}\boldsymbol{S}_{x,y}[\boldsymbol{H}_{\mathrm{o}}^{-1}\boldsymbol{R}^{-1}]\boldsymbol{R}\boldsymbol{S}_{x,y}.$$

As in the above example, the term in brackets is the inverse of $\boldsymbol{E}_{\mathrm{fPo}}$. Letting $\boldsymbol{R}\boldsymbol{S}_{x,y} = \boldsymbol{S}_{1,2}$, i.e. reflections about the $45°$ ($\boldsymbol{R}\boldsymbol{S}_x$) or $-45°$ ($\boldsymbol{R}\boldsymbol{S}_y$) lines, $\boldsymbol{E}_{\mathrm{fPo}}$ is seen to be symmetric to its inverse with respect to reflections about either the $45°$ or $-45°$ lines:

$$\boldsymbol{E}_{\mathrm{fPo}} = \boldsymbol{S}_{1,2}\boldsymbol{E}_{\mathrm{fPo}}^{-1}\boldsymbol{S}_{1,2}.$$

This flow possesses ordinary symmetry as well. The horizontal flow with $v(\xi)$ odd is symmetric with respect to $180°$ rotations about the origin:

$$\boldsymbol{H}_{\mathrm{o}} = \boldsymbol{R}^2\boldsymbol{H}_{\mathrm{o}}\boldsymbol{R}^2.$$

Additionally, $90°$ rotations possess the same symmetry; that is:

$$\boldsymbol{R} = \boldsymbol{R}^2\boldsymbol{R}\boldsymbol{R}^2.$$

Therefore, $\boldsymbol{R}\boldsymbol{H}_{\mathrm{o}} = [\boldsymbol{R}^2\boldsymbol{R}\boldsymbol{R}^2][\boldsymbol{R}^2\boldsymbol{H}_{\mathrm{o}}\boldsymbol{R}^2]$. But since $\boldsymbol{R}^4 = \boldsymbol{1}$, this means that $\boldsymbol{E}_{\mathrm{fPo}}$ itself is symmetric with respect to $180°$ rotations about the origin:

$$\boldsymbol{E}_{\mathrm{fPo}} = \boldsymbol{R}^2\boldsymbol{E}_{\mathrm{fPo}}\boldsymbol{R}^2.$$

The orientation preserving map with $\boldsymbol{H}$ odd possesses both ordinary and time reversal symmetry. A summary of the symmetry information appears in table 2. An important point to reiterate here is that all the analysis, and hence tables 1 and 2, are independent of the exact functional form for the velocity field. All that has been specified is the even or oddness of $v(\xi)$. The analysis turns out to be useful because other periodic flows fit into the same general framework. In fact, the analysis is not limited to two-dimensional time-periodic flows, but can also be extended to three-dimensional spatially periodic duct flows, as shall be illustrated in §7.

5. Island symmetry

Particles located on periodic points return exactly to their initial location after an integer number of iterations. (The eggbeater flow, essentially a flow on a T^2-torus, does not have to have periodic points (see Grebogi *et al.* 1985).) As an illustration consider the eggbeater flow with $T = 0.4$, and its corresponding Poincaré section, shown in figure 3*a*. If we place a line of particles inside one of the islands, and convect the line for four periods, the collection of particles returns approximately to its initial condition (figure 5). Clearly, there is some particle, located in the interior of the

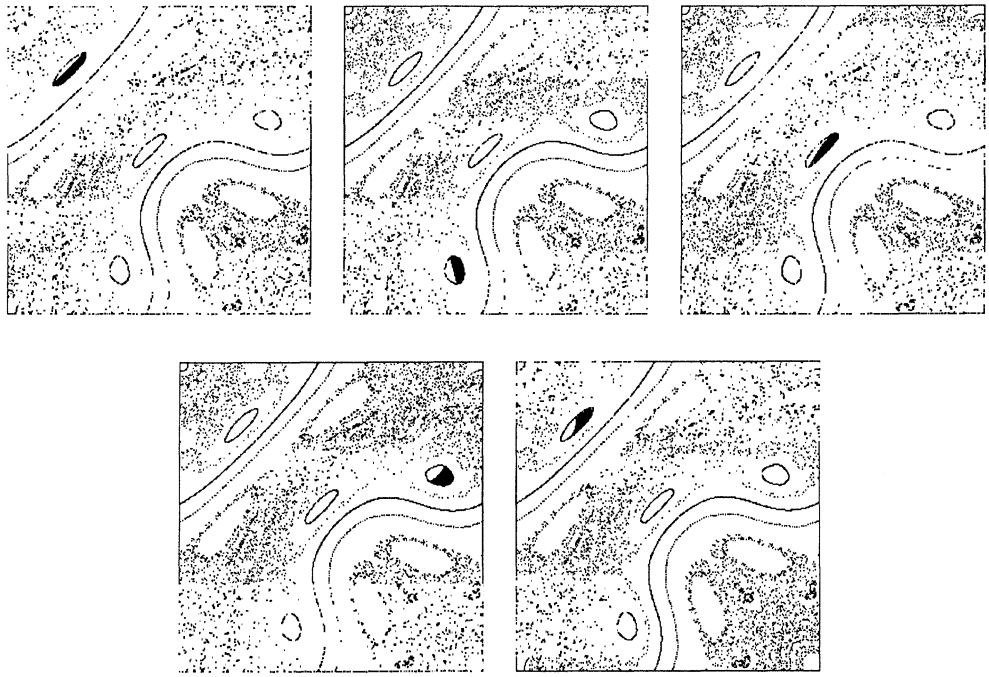

Figure 5. Motion of a period-four island. A dividing line with endpoints at $(-0.7, 0.5)$ and $(-0.5, 0.7)$ is placed in the interior of the island; the contents of the island are shown in black and white. Starting at the top and reading from left to right, the figures show the island appearance after zero, one, two, three, and four periods. Note the relatively small twist within the island.

island, which returns exactly to its initial location. A periodic point is formally defined as a point which returns exactly to its initial location after a specified number of iterates of the mapping, but not before, i.e. $\boldsymbol{z}$ is a periodic point of order n of the map $\boldsymbol{M}$ if $\boldsymbol{z} = \boldsymbol{M}^k\boldsymbol{z}$ for $k = n$ but not $k < n$. Obviously, if one point is n-periodic, then there are $n-1$ other points which are also n-periodic.

The location and character of periodic points are one possible way of characterizing a mapping. Periodic points can be classified as either elliptic or hyperbolic, depending on the motion which occurs near them. Motion near hyperbolic points consists of extension and compression and is characterized by exponential length stretch. A closed flow which contained only hyperbolic points would mix very well. However, in most cases, elliptic points are inevitable. The motion near elliptic points is rotational, and is characterized by linear length stretch; typically, the rate of stretch is negligible as compared with that produced by hyperbolic points. Furthermore, elliptic points are usually surrounded by invariant closed curves (as consequence of the KAM theorem (see Guckenheimer & Holmes 1983). Any particle which is initially bounded by an invariant curve remains bounded for all time. The presence of elliptic points and invariant curves has a negative impact on mixing. Fluid which is located inside a closed invariant curve is unable to mix with fluid outside it. The outermost invariant curve of an elliptic periodic point is in fact the island boundary.

Flows which exhibit symmetry have special behaviour with regard to the location of their periodic points: the points are always found in symmetric pairs. That is, if a map contains a periodic point at $\boldsymbol{x}$, then a periodic point is also located at $\boldsymbol{S}^{-1}\boldsymbol{x}$. The proof is as follows. A periodic point is defined as $\boldsymbol{x} = \boldsymbol{M}^k\boldsymbol{x}$. Say that $\boldsymbol{M}$ possesses

time-reversal symmetry, i.e. $\boldsymbol{M} = \boldsymbol{S}\boldsymbol{M}^{-1}\boldsymbol{S}^{-1}$. Upon substituting for $\boldsymbol{M}$ in the above expression, we obtain

$$\boldsymbol{x} = (\boldsymbol{S}\boldsymbol{M}^{-1}\boldsymbol{S}^{-1})^k\boldsymbol{x} = \boldsymbol{S}\boldsymbol{M}^{-k}\boldsymbol{S}^{-1}\boldsymbol{x}.$$

Pre-multiplying by $\boldsymbol{S}^{-1}$ yields $\boldsymbol{S}^{-1}\boldsymbol{x} = \boldsymbol{M}^{-k}\boldsymbol{S}^{-1}\boldsymbol{x}$. Letting $\boldsymbol{x}' = \boldsymbol{S}^{-1}\boldsymbol{x}$, then $\boldsymbol{x}' = \boldsymbol{M}^{-k}\boldsymbol{x}'$ and therefore $\boldsymbol{x}'$ is also a periodic point of $\boldsymbol{M}$. The same relationship can be found to hold utilizing the definition of ordinary symmetry. Thus, for example, if the symmetry is a reflection, we know that all periodic points, and hence all islands, must exist along the line of symmetry, or in pairs on opposite sides of the line. Although we might not know the character of the periodic points, having a gross idea of their location in the flow, via their symmetries, provides an important basis for the elimination of islands.

6. Symmetry manipulation

The overall goal of practical mixing process is to accomplish the most mixing in the least time (or consuming the least energy, etc.). For fluid systems in which surface tension and molecular diffusion are negligible, this means finding a fluid flow (fluid motion) which is best able to create intermaterial area between species, i.e. stretch material interfaces. Unfortunately, there is no feasible means to predict *a priori* what is the 'best' motion for accomplishing this task, except for trial and error. That is, perform the experiment, or numerical simulation, involving the flow in question, and determine if this meets the desired criteria.

The problem becomes simpler if we impose a set of restrictions. For example, we could restrict the search to periodic protocols (e.g. ... $\boldsymbol{VHVHVH}$), and then the problem reduces to finding the optimal period of operation. Another approach might be to fix the period of operation, but then find the protocol which produces the best mixing. In the context of the eggbeater flow, the question can be posed simply as: What is the sequence of horizonal and vertical flows which yield the best mixing? Unfortunately, finding the true optimal solution to this problem appears to be beyond current computational capabilities (Franjione & Ottino 1987).

It is in this framework that information such as the symmetry of flows is most useful. Symmetries do not supply quantitative information; instead they provide geometrical constraints on the motion. We now focus on the task of using these symmetry constraints to suggest a sequence of flows which yields the best mixing. As outlined above, however, we wish to devise a means for accomplishing this goal without resorting to a detailed reconstruction of the flow (either numerically or experimentally). The approach is as follows. Since it is true that all periodic points, and hence all islands, will be found in symmetric arrangements in the flow field, one simple and intuitive way to enable fluid to experience both 'good' and 'poor' mixing flows is to alter the flow systematically so that island positions are shifted. In essence, we are restricting the optimization problem, so that now we focus only on combining periodic protocols. In this way, fluid which was previously trapped inside an island might now be found in a well-mixed region. Exact knowledge of the island size and location is not required, however, since all we want to do is shift their positions.

As an illustration, consider the flow shown in figure 3*a*, i.e. the flow $\boldsymbol{VH}$ (with the even $v(\xi)$) with $V_s = 0$ and $T = 0.4$. We have shown that this flow possesses time reversal symmetry with respect to reflections about the $-45°$ line, indicating that any islands in the flow should be found on this line, or in pairs on opposite sides of the line. One way that mixing in this flow might be enhanced is to run a flow in which

PHILOSOPHICAL TRANSACTIONS OF THE ROYAL SOCIETY A MATHEMATICAL, PHYSICAL & ENGINEERING SCIENCES

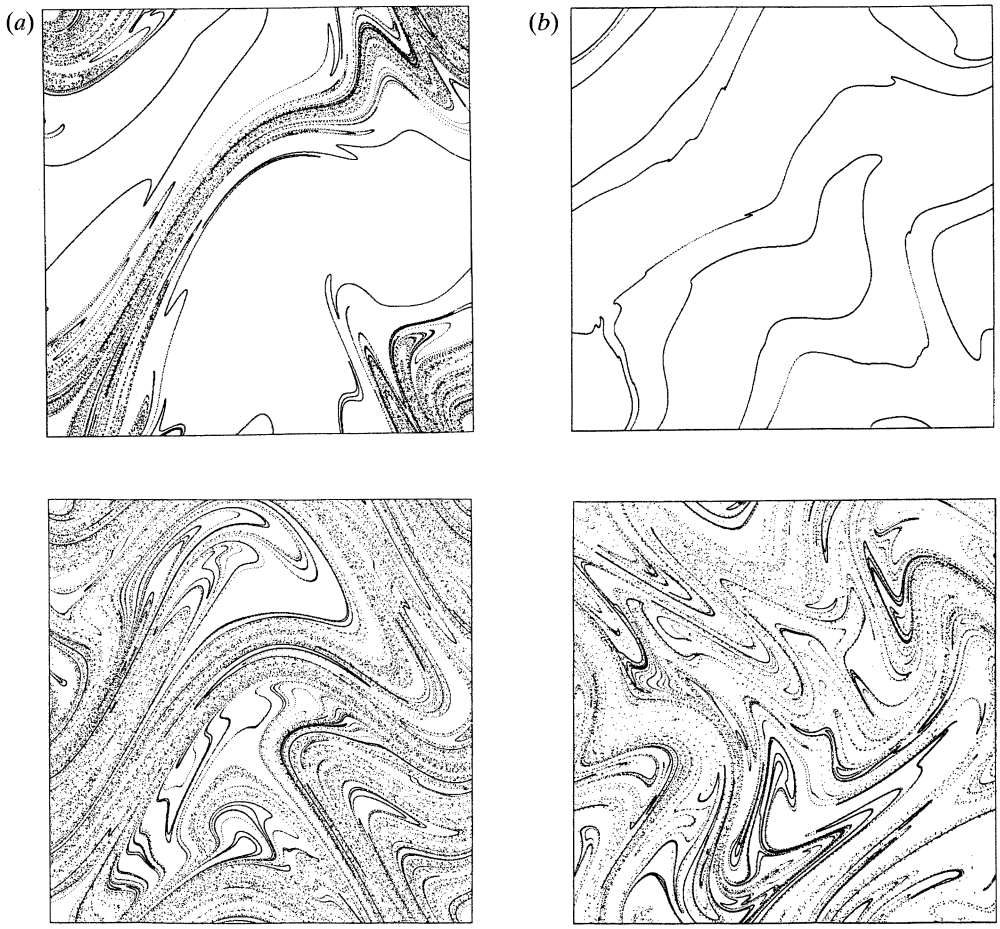

Figure 6. Application of the recursive algorithm to eggbeater flow. Initial condition for all figures was a line of 50000 points at $x = -0.9$. (*a*) $V_s = 0$, $T = 0.4$. The periodic protocol, $16 \times VH$, is compared with the corresponding 32 symbol recursive protocol. (*b*) $V_s = 0.55$, $T = 0.7$. The periodic protocol, $32 \times VH$ is compared with the corresponding 64-symbol recursive protocol.

the island positions are the same, but reflected across the 45° line, i.e. the flow $\boldsymbol{S}_1[\boldsymbol{VH}]\boldsymbol{S}_1 = \boldsymbol{HV}$. A naive interpretation might suggest that operating these two sequences in an alternating fashion could achieve the desired object. However, this is not necessarily the case since a periodic flow field consisting of $\boldsymbol{HVVH}$ can be shown to possess a 180° rotational symmetry. Therefore, to enhance any poor mixing created by this flow, we apply the same logic, and run the sequence of flows in which the island positions are reflected across the 45° line, i.e. the flow $\boldsymbol{S}_1[\boldsymbol{HVVH}]\boldsymbol{S}_1 = \boldsymbol{VHHV}$. The key concept behind this method of choice of flow sequences is to choose the next flow sequence which will (in principle) destroy any islands which were created by the entire preceding sequence. This idea can be stated symbolically as follows:

$$\boldsymbol{x}_{n+1} = \boldsymbol{P}_n \boldsymbol{x}_n, \quad \boldsymbol{P}_{n+1} = \boldsymbol{f}(\boldsymbol{P}_n).$$

We call a sequence created using a set of rules such as these a *recursive* sequence. The first equation indicates where the particle, which was initially located at $\boldsymbol{x}_n$, will be found after the action of flow sequence $\boldsymbol{P}_n$. The second equation indicates how the flow

sequence is to be modified. For a periodic sequence, this rule for generation of the flow sequence is simply $\boldsymbol{P}_{n+1} = \boldsymbol{P}_n$. In the discussion above, we used the rule

$$\boldsymbol{P}_{n+1} = \boldsymbol{S}_1 \boldsymbol{P}_n \boldsymbol{S}_1 \boldsymbol{P}_n$$

which was based on the concept of manipulating the symmetry, and hence the island positions, by reflection across the 45° line. In some sense, we are implementing a control scheme. However, it is not a feedback system, as in such a case, the control action would be based on the 'state variable' $\boldsymbol{x}$, the positions of fluid particles in the flow. It is not a feedforward control system either, though, as in that case, the control action would be based on a predictive model for $\boldsymbol{x}$. In this scheme, the control action is based on the geometrical constraints of the fluid motion, i.e. the symmetries of the flow.

Let us now focus again on the specific case of enhancing mixing in the flow of figure 3*a*. In the figure 6*a* we show the appearance of a line of 10000 particles, initially at $x = -0.9$, and compare the mixing resulting from the periodic and recursive protocols. The mixing due to the recursive is much better. In figure 6*b*, we show the enhancement in mixing achieved for a different set of flow parameters. We see again the substantial improvement that is possible using the recursive protocol.

7. Application to duct flows

It is apparent that simple geometric analysis can give clues to the mixing behaviour, and provides also a means for determination of flow sequences leading to efficient mixing. So far, our analysis has encompassed two-dimensional time-periodic flows. However, many 'real' flows and systems of engineering interest are three dimensional and continuous (fluid is fed at an inlet and removed at a downstream outlet). In this section, we apply some of the methods to the investigation of a class of flows which are called chaotic duct flows.

Duct flows are open isochoric flows which are comprised of a two-dimensional cross-sectional flow augmented by a unidirectional axial flow. Generally, fluid is mixed in the cross section while it is simultaneously transported down the duct axis. In a 'regular' duct flow, i.e. one in which the cross-sectional and axial flows are independent of both time and distance along the duct axis, material lines stretch linearly in time (Franjione & Ottino 1991), a characteristic of a poor mixing flow. For a duct flow to exhibit good mixing, it is necessary that the flow contain some degree of reorientation. The shape of the stream surfaces must change either in time or along the duct axis. An experimental study of time- and spatially periodic chaotic duct flows is presented by Kusch & Ottino (1992).

We study the mixing in a prototype spatially periodic duct flow called the *partitioned-pipe mixer* (PPM). This flow was first introduced by Khakhar *et al.* (1987) and consists of a pipe partitioned into a sequence of semicircular ducts by means of orthogonally placed rectangular plates (see figure 7). A cross-sectional motion is induced through rotation of the pipe wall at constant speed relative to the assembly of plates, and the axial flow is caused by an axial pressure gradient. The reorientation in this flow occurs in the axial spatial dimension. At every length L along the pipe axis, the orientation of the dividing plate shifts by 90°.

We assume that the cross-sectional and axial velocities are independent from one another. The cross-sectional velocity field may be found by solving the biharmonic equation for the streamfunction, while the axial velocity is found by solution of a

PHILOSOPHICAL TRANSACTIONS OF THE ROYAL SOCIETY A MATHEMATICAL, PHYSICAL & ENGINEERING SCIENCES

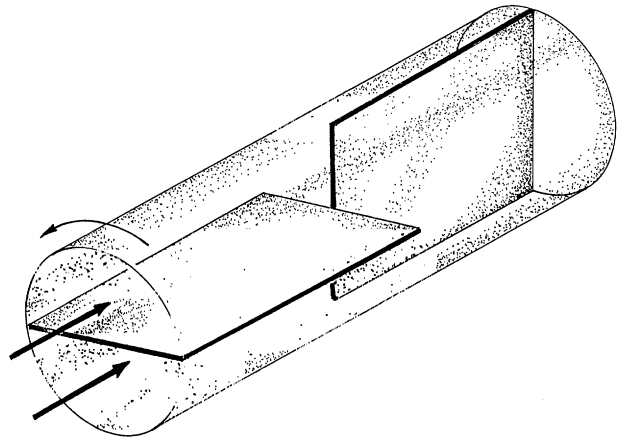

Figure 7. Spatially periodic duct flow, the partitioned-pipe mixer.

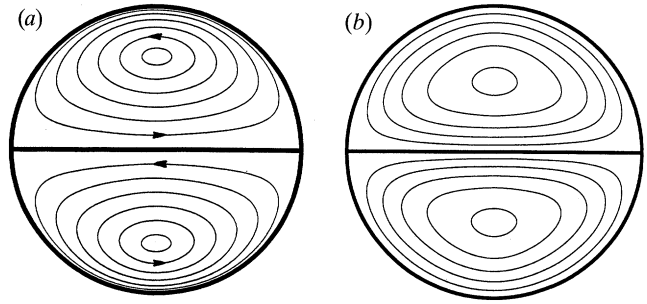

Figure 8. (*a*) Cross-sectional streamlines and (*b*) axial velocity contours in the PPM.

Poisson equation. An exact solution exists for the axial velocity (Berker 1960); for the cross-section velocity, we use an approximate solution due to Khakhar (1986). The non-dimensionalized equations of the velocity field are:

$$v_r = \beta r(1-r^{\nu})\sin 2\theta,$$

$$v_\theta = -\beta r\{2-(2+\nu)\,r^{\nu}\}\sin^2\theta,$$

$$v_z = \frac{16\pi}{\pi^2-8}\sum_{k=1}^{\infty}\{r^{2k-1}-r^2\}\frac{\sin[(2k-1)\theta]}{(2k-1)\{4-(2k-1)^2\}},$$

where (r,θ,z) are the usual cylindrical coordinate variables and β is a 'mixing strength parameter', which is effectively equal to the ratio of the cross-sectional and axial strain rates. The cross-sectional streamlines, along with the axial velocity contours are shown in figure 8.

For spatially periodic systems, Poincaré sections are constructed by marking the particle position in the cross section when the particle reaches the end of a spatially periodic unit. The cross-sectional mapping in the PPM can be viewed as four distinct submappings: (i) helical flow in a semicircular duct; (ii) rigid body rotation by 90° about the pipe centre; (iii) a second helical flow; (iv) rigid body rotation of −90° back to its initial orientation. Letting $\boldsymbol{F}_0$ represent the mapping of particle position from the front to the back of a semicircular duct, the overall mapping in the periodic unit can be expressed as

$$\boldsymbol{x}_{n+1} = \boldsymbol{R}^{-1}\boldsymbol{F}_0\boldsymbol{R}\boldsymbol{F}_0\boldsymbol{x}_n = \boldsymbol{T}\boldsymbol{x}_n.$$

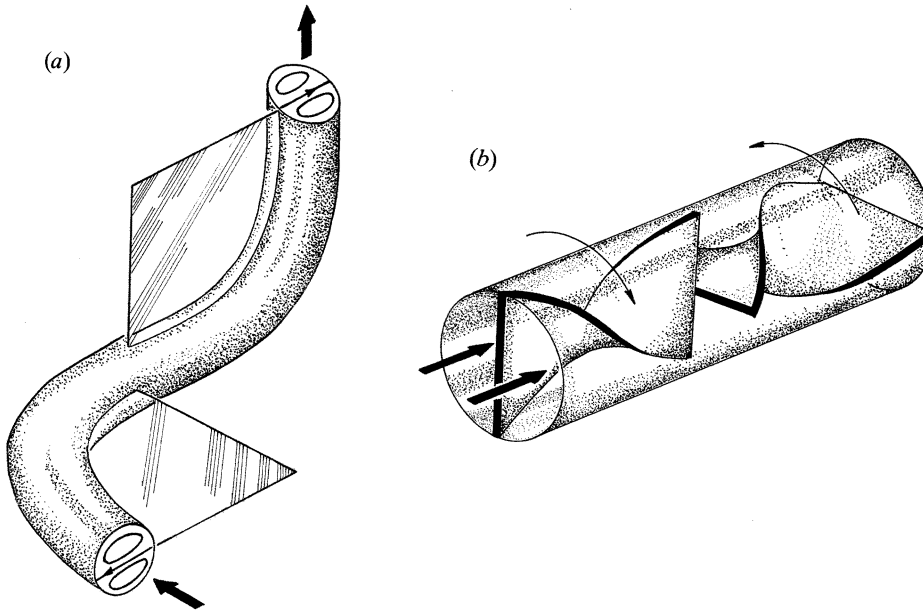

Figure 9. (*a*) Twisted pipe flow of Jones *et al.* (1989). (*b*) The Kenics® static mixer.

Let us investigate the symmetry properties of $\boldsymbol{F}_o$, and of $\boldsymbol{T}$. From the streamline portrait, it is apparent that $\boldsymbol{F}_o$ possesses two time-reversal symmetries and ordinary symmetry. If the portrait is reflected across either the x- or y-axis, the inverse motion results. That is:

$$\boldsymbol{F}_o = \boldsymbol{S}_{x,y}\boldsymbol{F}_o^{-1}\boldsymbol{S}_{x,y}.$$

Additionally, the portrait is invariant to 180° rotations:

$$\boldsymbol{F}_o = \boldsymbol{R}^2\boldsymbol{F}_o\boldsymbol{R}^2.$$

Note that these symmetries are identical to those of the horizontal shear flow with a velocity field which is odd about the origin. The symmetries of the overall PPM motion can therefore be found from tables 1 and 2. That is, there are eight other combinations of $\boldsymbol{F}_o$, $\boldsymbol{F}_o^{-1}$, and 90° and −90° rotations which would yield equivalent Poincaré sections. This particular flow, $\boldsymbol{T}$, possesses two time reversal symmetries (reflection about the 45° and −45° lines), and one ordinary symmetry (rotation by 180°).

There are other spatially periodic flows which fit into this framework, some of which have been investigated in detail, although in a different context. The flow in a sequence of curved pipes has been studied by Jones *et al.* (1988). In this device, cross-sectional mixing is induced by inertial forces, in the form of two secondary vortices which rotate in opposite directions. Fluid is pushed down the pipe by an axial pressure gradient. When different segments of curved pipe are fitted together (figure 9*a*), the relative position of the vortices in adjacent segments change, resulting in chaotic fluid particle trajectories, and enhanced mixing. This device shall be referred to as the 'T-mixer'. The Kenics® static mixer is a chaotic duct flow which utilizes a helical twisting of a diametrically placed duct boundary to induce a cross-sectional flow, while the axial flow is caused by a pressure gradient. Reorientation is promoted by fitting the helical segments together in a non-smooth fashion (figure

PHILOSOPHICAL TRANSACTIONS OF THE ROYAL SOCIETY A MATHEMATICAL, PHYSICAL & ENGINEERING SCIENCES

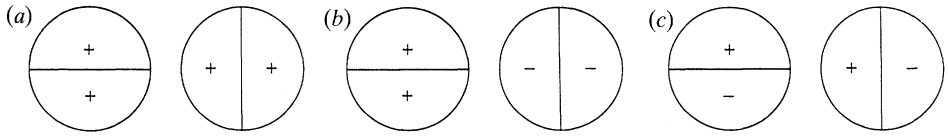

Figure 10. Topological differences among cross-sectional flows in adjacent elements in the (*a*) PPM, (*b*) K-mixer, and (*c*) T-mixer. A '+' indicates that the sense of rotation is counter-clockwise, while a '−' indicates clockwise rotation.

9*b*). We refer to this device as the 'K-mixer'. Actually, the cross-sectional flows in these two devices are similar to those in the partitioned-pipe mixer, in that all three contain two recirculating regions which are located on opposite sides of the pipe (for the K-mixer, this requires that we view the motion in a coordinate system based on the unwound helix). However, there are some important topological differences. In the PPM, the sense of rotation of these two recirculating regions is identical, and the sense of rotation in adjacent elements is also identical. In the T-mixer, the sense of rotation in the two regions is opposite, but the rotation in adjacent elements is identical. In the K-mixer, the rotation in the two recirculating regions is the same, but the rotation in adjacent elements is opposite. This is represented schematically in figure 10. These mixers cover three out of the four possible alternatives involving symmetrically positioned vortices and 90° rotations.

The framework for analysis is identical to that established earlier for the eggbeater flows. The cross-sectional motion of the T-mixer possesses time reversal symmetry with respect to reflections across the y-axis and 180° rotations about the origin, and ordinary symmetry with respect to reflections across the x-axis. Letting $\boldsymbol{F}_{\mathrm{e}}$ represent the cross-sectional motion in an element of the T-mixer, these symmetries can be written as

$$\boldsymbol{F}_{\mathrm{e}} = \boldsymbol{S}_y \boldsymbol{F}_{\mathrm{e}}^{-1} \boldsymbol{S}_y, \quad \boldsymbol{F}_{\mathrm{e}} = \boldsymbol{R}^2 \boldsymbol{F}_{\mathrm{e}}^{-1} \boldsymbol{R}^2, \quad \boldsymbol{F}_{\mathrm{e}} = \boldsymbol{S}_x \boldsymbol{F}_{\mathrm{e}} \boldsymbol{S}_x.$$

Since these are identical to the symmetries in the EBF with $v(\xi)$ even, the symmetries of the composite mappings can be found in table 2. There are only two distinct T-mixer flows, and these correspond to $\boldsymbol{F}_{\mathrm{Pe}}$ and $\boldsymbol{F}_{\mathrm{Re}}$.

The cross-sectional motion for a single element of the K-mixer is the same as that for the PPM ($\boldsymbol{F}_{\mathrm{o}}$). However, the sense of rotation is opposite in adjacent elements. We write the overall motion in the K-mixer as

$$\boldsymbol{x}_{n+1} = \boldsymbol{R}^{-1} \boldsymbol{F}_{\mathrm{o}}^{-1} \boldsymbol{R} \boldsymbol{F}_{\mathrm{o}} \boldsymbol{x}_n = \boldsymbol{T}_{\mathrm{K}} \boldsymbol{x}_n.$$

This is a similar composition of flows and rotations as that of the eggbeater flow $\boldsymbol{E}_{0,0011}$. Because the symmetries of the submappings are identical to those in the eggbeater flow (with $v(\xi)$ odd), then the symmetries of the composite mapping are identical also. The K-mixer flow thus possess time-reversal symmetry with respect to 90° and −90° rotations, and ordinary symmetry with respect to 180° rotations. Additionally, the K-mixer can be found to be given by an orientation reversing fundamental mapping, $\boldsymbol{E}_{\mathrm{Ro}}$.

We wish to compare the mixing behaviour in the PPM, T-mixer, and K-mixer by comparing their Poincaré sections. Although the flows in the three mixers are qualitatively similar, their topologies, and thus their symmetries, are quite different. For an exact, quantitative study, we would need to determine the flow in each mixer, and base the Poincaré section on this velocity field. However, to isolate the effect of topology, we compute and compare Poincaré sections based on the mappings for the individual mixers, while using the PPM streamlines for all three mixers. Henceforth,

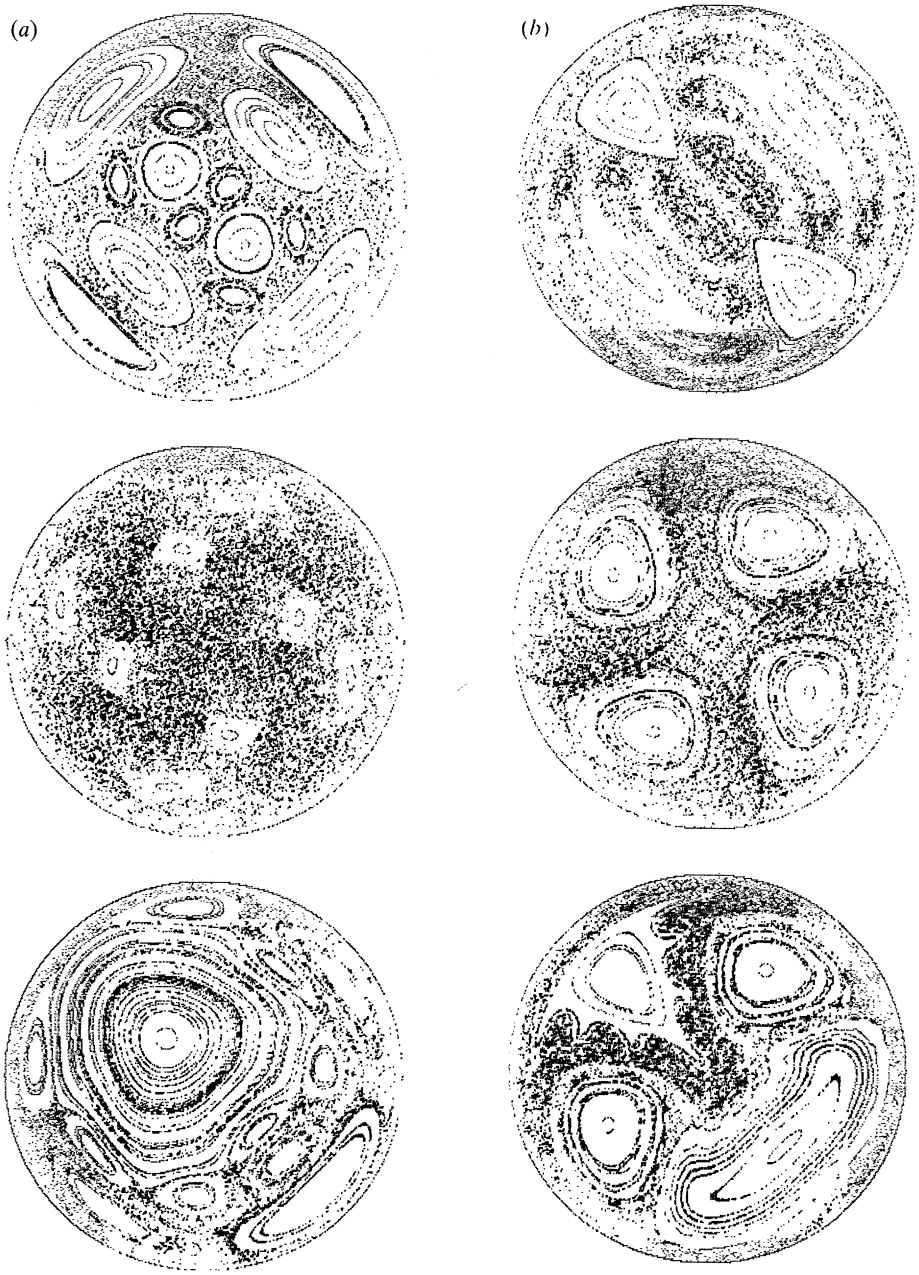

Figure 11. Poincaré sections in the PPM (top), K-mixer (middle), and T-mixer (bottom). (a) $\beta = 2$; (b) $\beta = 6$.

we will continue to refer to the K- and T-mixers with the understanding that these terms refer to the flows described by the PPM velocity field with the appropriate topology. These Poincaré sections are compared in figure 11. For a given value of β, the K-mixer exhibits the best cross-sectional mixing. It also appears that the T-mixer mixer exhibits behaviour which is intermediate between the K-mixer and the PPM. (It is probably unfair to the PPM to compare all three mixers at the same values

PHILOSOPHICAL TRANSACTIONS OF THE ROYAL SOCIETY A MATHEMATICAL, PHYSICAL & ENGINEERING SCIENCES

of β. In the PPM, β can be varied, whereas in the T-mixer, β is clearly a consequence of the strength of the secondary flow, and is therefore fixed for a given T-mixer geometry. An actual comparison based on experimental data would most likely involve a low value β for the T-mixer.) The Poincaré sections for the T-mixer flow display some features which are contained in the PPM and some which are present in the K-mixer. Consider, for example, the set of Poincaré sections for $\beta = 6$, shown in figure 11*b*. The island in the upper left quadrant of the T-mixer flow, with its wavy outer boundary, is strikingly similar to the islands located on the $-45°$ line in the PPM. The pair of islands on either side of the 45° line in the T-mixer flow also appear in the K-mixer flow.

Earlier, we saw how identification and manipulation of symmetry in the eggbeater flow yields a systematic means for achieving enhanced mixing. Here, we consider symmetry manipulation in the partitioned-pipe mixer, and study the results in terms of Poincaré sections. We adopt the following notation. The PPM flow can be written as sequence involving two separate flows: one in which the dividing plate has a horizontal orientation, and one in which the plate is oriented vertically. We denote these two flows as $\boldsymbol{H}$ and $\boldsymbol{V}$ respectively. The 'standard' PPM flow is simply an alternating sequence of 'horizontal' and 'vertical' flows. The base protocol, $\boldsymbol{P}_0$, is given by:

$$\boldsymbol{P}_0 = \boldsymbol{VH}.$$

Note that, as with the eggbeater flow, the horizontal and vertical flows are related by

$$\boldsymbol{V} = \boldsymbol{RHR}^{-1}.$$

Because this flow is identical, geometrically, to the orientation preserving eggbeater flow with $v(\xi)$ odd, we know that this flow possesses two time-reversal symmetries, reflections about the 45° and $-45°$ lines. Here, we 'rotate the flow' by 90°; that is, follow the flow $\boldsymbol{VH}$ with $\boldsymbol{R}[\boldsymbol{VH}]\boldsymbol{R}^{-1} = \boldsymbol{HV}$. In the $\boldsymbol{HV}$ flow, then, the two symmetry lines will switch places relative to their positions in the $\boldsymbol{VH}$ flow, i.e. what structures were before located on the 45° line in the $\boldsymbol{VH}$ flow could be found on the $-45°$ line in the $\boldsymbol{HV}$ flow. The recursion relation between the current and the subsequent protocol can be written as

$$\boldsymbol{P}_{n+1} = \boldsymbol{RP}_n\boldsymbol{R}^{-1}\boldsymbol{P}_n.$$

The sequence generated is a Morse–Thue sequence. Poincaré sections for $\beta = 2$ and

$$n = 0\,(\boldsymbol{VH}),$$

$$n = 1\,(\boldsymbol{HVVH}),$$

$$n = 2\,(\boldsymbol{VHHVHVVH})$$

and

$$n = 3\,(\boldsymbol{HVVHVHHVVHHVHVVH})$$

are shown in figure 12. The Poincaré sections are constructed by choosing n, and then using $\boldsymbol{P}_n$ as the mapping. It is apparent that the mixing for the $\boldsymbol{P}_3$ protocol is the best one, and presumably, using the $\boldsymbol{P}_4$ protocol would improve the mixing even further. Similar enhancement of mixing is seen when the recursive protocol is utilized in the K- and T-mixers. As the number of units in the recursive sequence is increased, the extent of the mixing increases, as both the number and size of islands decreases.

It is important to realize, however, that a Poincaré section is a long-time picture of the mixing behaviour (i.e. resulting from a mixer with an infinite number of

PHILOSOPHICAL TRANSACTIONS OF THE ROYAL SOCIETY A MATHEMATICAL, PHYSICAL & ENGINEERING SCIENCES

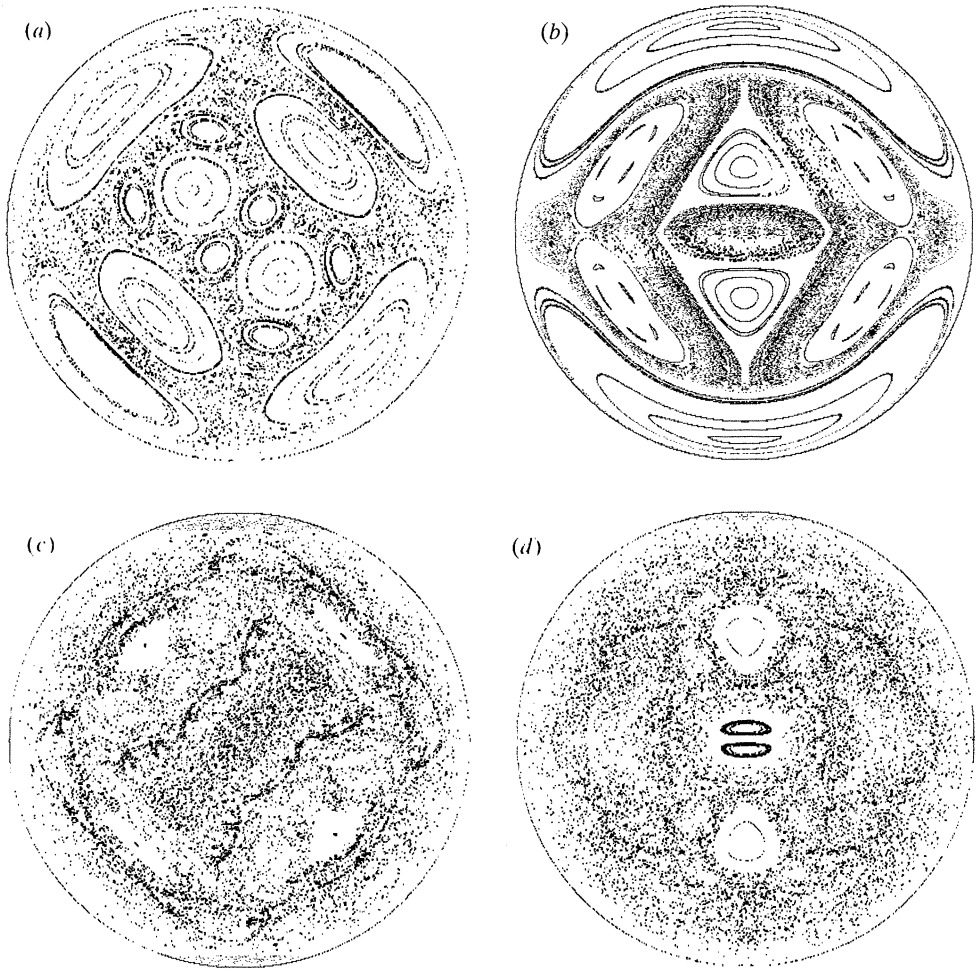

Figure 12. Poincaré sections for PPM after symmetry manipulations for $\beta = 2$. (*a*) ***VH***; (*b*) ***HVVH***; (*c*) ***VHHVHVVH***; (*d*) ***HVVHVHHVVHHVHVVH***.

elements), and it is therefore an upper bound on the extent of mixing which can occur for a particular protocol. In contrast, a mixing device used in practical applications will have a finite length, and the mixing will not necessarily appear so effective. The extent of the cross-sectional mixing is best visualized by examining the dispersion of marked particles, as was done for the eggbeater flow. However, rather than present all of these results, we simply state that mixing achieved in a finite length mixer which uses a recursive sequence of elements is always better than that achieved in a mixer which uses a periodic sequence.

8. Conclusions

Symmetries are a useful analytical tool because they are based on only the simplest geometrical characteristics of a flow; detailed information is not needed. Such information provides means of classifying flows. Indeed, in this paper, we have characterized a family of two-dimensional flows, as well as a family of three-

Figure 13

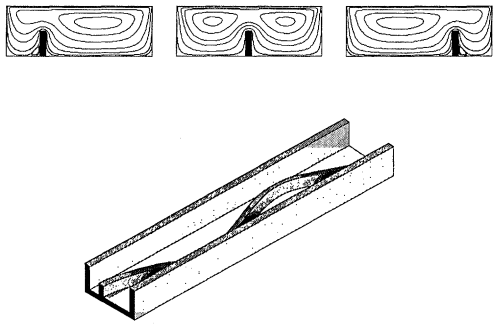

Figure 14

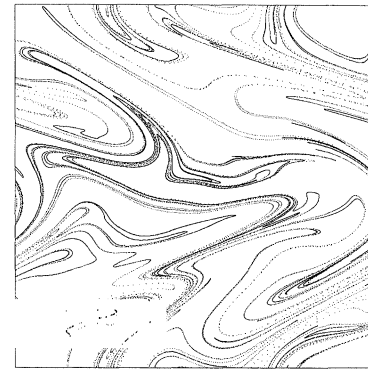

Figure 13. Generation of a time-dependent change in the geometry of a two-dimensional cavity flow by a spatially dependent change in the geometry of the cross section of the corresponding duct flow. Cross-sectional and axial motions are caused by a diagonally moving lid, which is not shown. The top part of the figure computed cross-sectional streamlines corresponding to three different axial locations. Although in the figure the 'snake baffle' is spatially periodic, it could be utilized as an aperiodic recursively generated shape as well.

Figure 14. Mixing in the eggbeater flow achieved utilizing the 'Fibonacci' protocol. All figures utilize $v(\xi)$ even with $V_s = 0$ and $T = 0.4$. The initial state is a line of 50000 particles placed along $x = -0.9$. Compare with figure 6*a*.

dimensional duct flows, in terms of their symmetry properties. Furthermore, symmetries provide a global, rather than a local, picture of the mixing. We have shown how this global picture can be utilized to devise effective mixing protocols, i.e. sequences of flows which generate efficient mixing, for both time periodic two-dimensional flows and spatially periodic three-dimensional flows. Although results are shown for only a few parameter values, we have found in general that mixing produced by the recursive protocol is always better than the corresponding time periodic protocol. We have found this to be true for other flows as well (see Franjione *et al.* 1989).

All of the flows discussed in this paper are discontinuous, in that the overall flows were composed of discrete parts which were fused together in a non-smooth fashion. However, symmetries can be deduced for continuously varying flows as well. Symmetry is found by consideration of the velocity field, rather than the motion, although the definition of symmetry is identical (Leong & Ottino 1989). A recursive protocol for such a continuous system, based on the manipulation of the symmetries, would be similar to that of a discontinuous one. For example, the ideas presented in terms of the cavity flow in Franjione *et al.* (1989) can be extended continuous motion of walls. Moreover, the methodology for continuously varying flows can be utilized for duct flows. Flows in cavities with internal moving baffles can be used to generate continuous throughput mixing flows; a 'snake baffle' in a channel with a diagonally moving lid is just one example (see figure 13).

One could imagine a host of other flows for which an analysis of symmetries could provide important information for subsequent enhancement of mixing. Examples include variations of the Rayleigh–Bénard flow as well as flows able to generate effective mixing based on inertial effects (Sobey 1985). However, possessing symmetry is not enough. In many cases, as for example in the two-dimensional journal bearing flow (Swanson & Ottino 1990; Chaiken *et al.* 1986), a flow may not

PHILOSOPHICAL TRANSACTIONS OF THE ROYAL SOCIETY A MATHEMATICAL, PHYSICAL & ENGINEERING SCIENCES

have enough symmetries as to be able to shift or rotate them to generate effective mixing.

Based on the examples presented in this paper, one might be tempted to draw the conclusion that flows which possess a rotational symmetry mix better than those with reflectional symmetry. This was especially apparent in duct flows, where the K-mixer was much more effective than either the PPM or T-mixer for same values of β. However, it is important to stress that this phenomenon is not entirely general. For example, mixing in the *blinking vortex* flow with co-rotating vortices, a flow which possesses reflectional symmetry, is much better than in the same flow with counter-rotating vortices, a flow which possesses rotational symmetry (Khakhar *et al.* 1986). Thus an examination of the mixing abilities of flows cannot rely on symmetries alone and needs to be augmented with other analyses. An exact determination of the placement and character of periodic points would be the best course of action.

The class of mixing protocols leading to effective mixing can be augmented as well. The protocols presented in this paper are just but one possibility. As stated in §6, the protocols studied in this work can be expressed symbolically as:

$$\boldsymbol{x}_{n+1} = \boldsymbol{P}_n \boldsymbol{x}_n, \quad \boldsymbol{P}_{n+1} = \boldsymbol{f}(\boldsymbol{P}_n),$$

where $\boldsymbol{P}_n$ is the current flow sequence, and the 'rule' $\boldsymbol{f}(\cdot)$ describes how to obtain the next sequence. For the recursive protocol discussed in this paper, the rule is based on symmetry considerations. However, other rules are possible. For example, consider

$$\boldsymbol{P}_{n+2} = \boldsymbol{P}_n \boldsymbol{P}_{n+1}$$

with $\boldsymbol{P}_1 = \boldsymbol{H}$ and $\boldsymbol{P}_2 = \boldsymbol{VH}$. We refer to a sequence generated with these rules as the 'Fibonacci sequence' (this idea was suggested by R. S. MacKay). Figure 14 shows mixing in the eggbeater flow using this sequence for the same conditions as in figure 6. The mixing appears comparable, and if anything, worse. A related question, which will no doubt occur to the reader, is the effectiveness of a *random* protocol. Any initial optimism regarding the effectiveness of such a protocol is tempered by two considerations; the first one is that the desired sequences of actions are relatively short, not nearly enough to reach results of statistical significance. The second is the difficulty of implementing the idea into industrial designs. Our results in fact suggest that although it is possible for a random protocol to result in effective mixing, it would also be possible for such a random protocol to yield poor mixing.

Finally, it should be noted that the recursive protocols which we studied here were based on combining sub-mappings $\boldsymbol{VH}$ and $\boldsymbol{HV}$, with the period of $\boldsymbol{H}$ and $\boldsymbol{V}$ being identical. However, other possibilities would allow $\boldsymbol{H}$ and $\boldsymbol{V}$ to possess different periods, or allow inverse motions, i.e. combinations involving $\boldsymbol{V}^{-1}\boldsymbol{H}$, $\boldsymbol{H}^{-1}\boldsymbol{V}$, etc. It is unclear whether these protocols would enhance mixing but they should be explored as well.

This work was supported by the National Science Foundation, under grant CTS-8909954. We thank Mr S. Jana for computing the cross-sectional flows shown in figure 13 (top) and to Dr C.-W. Leong for figure 13 (bottom).

References

Aref, H. 1990 Chaotic advection of fluid particles. *Phil. Trans. R. Soc. Lond.* A **333**, 273–288.

Berker, R. 1960 Intégration des équations du mouvement d'un fluid visqueux incompressible. In *Encyclopedia of physics*, vol. VIII/2 (ed. S. Flugge). Berlin: Springer-Verlag.

Chaiken, J., Chevray, R., Tabor, M. & Tan, Q. M. 1986 Experimental study of Lagrangian turbulence in a Stokes flow. *Proc. R. Soc. Lond.* A **408**, 165–174.

Chossat, P. & Golubitsky, M. 1988 Symmetry-increasing bifurcation of chaotic attractors. *Physica* D **32**, 423.

de Vogelaere, R. 1958 On the structure of symmetric periodic solutions of conservative systems, with applications. From *Contributions to the theory of non-linear oscillations IV* (ed. S. Lefschetz). Princeton University Press.

Franjione, J. G. & Ottino, J. M. 1987 Feasibility of numerical tracking of material lines and surfaces in chaotic flows. *Phys. Fluids* **30**, 3641–3643.

Franjione, J. G. & Ottino, J. M. 1991 Stretching in duct flows. *Phys. Fluids* A **3**, 2819–2821.

Franjione, J. G., Leong, C. W. & Ottino, J. M. 1989 Symmetries within chaos: a route to effective mixing. *Phys. Fluids* A **1**, 1772–1783.

Golubitsky, M., Stewart I. & Schaefer, D. G. 1985 *Singularities and groups in bifurcation theory*, vol. II. New York: Springer-Verlag.

Grebogi, C., Ott, E. & Yorke, Y. A. 1985 Attractors on an N-torus: quasiperiodicity vs. chaos. *Physica* D **15**, 354–373.

Greene, J. M., MacKay, R. S., Vivaldi, F. & Feigenbaum, M. J. 1981 Universal behaviour in families of area preserving maps. *Physica* D **3**, 468–486.

Guckenheimer, J. & Holmes, P. 1983 *Nonlinear oscillations, dynamical systems, and bifurcations of vector fields*. New York: Springer-Verlag.

Jones, S. W., Thomas, O. M. & Aref, H. 1989 Chaotic advection by laminar flow in a twisted pipe. *J. Fluid Mech.* **209**, 335–357.

Khakhar, D. V. 1986 *Fluid mechanics of laminar mixing: dispersion and chaotic flows*. Ph.D. thesis, University of Massachusetts.

Khakhar, D. V., Franjione, J. G. & Ottino, J. M. 1987 A case of chaotic mixing in deterministic flows: the partitioned-pipe mixer. *Chem. Engng Sci.* **42**, 2909–2926.

Khakhar, D. V., Rising, H. K. & Ottino, J. M. 1986 Analysis of chaotic mixing in two model systems. *J. Fluid Mech.* **172**, 419–451.

Kusch, H. A. & Ottino, J. M. 1992 Experiments on mixing in continuous chaotic flows. *J. Fluid Mech.* (In the press.)

Leong, C. W. & Ottino, J. M. 1989 Experiments on mixing due to chaotic advection in a cavity. *J. Fluid Mech.* **209**, 463–499.

Olver, P. J. 1986 *Applications of Lie groups to differential equations*. New York: Springer-Verlag.

Ottino, J. M. 1989*a* *The kinematics of mixing: stretching, chaos, and transport*. Cambridge University Press.

Ottino, J. M. 1989*b* The mixing of fluids *Sci. Am.* **260**, 56–67.

Sobey, I. J. 1985 Dispersion caused by separation during oscillatory flow through a furrowed channel. *Chem. Engng Sci.* **40**, 2129–2134.

Swanson, P. D. & Ottino, J. M. 1990 A comparative computational and experimental study of chaotic mixing of viscous fluids. *J. Fluid Mech.* **213**, 227–249.

Received 17 April 1991; revised 19 August 1991; accepted 18 September 1991

PHILOSOPHICAL TRANSACTIONS OF THE ROYAL SOCIETY A MATHEMATICAL, PHYSICAL & ENGINEERING SCIENCES

Figure 13

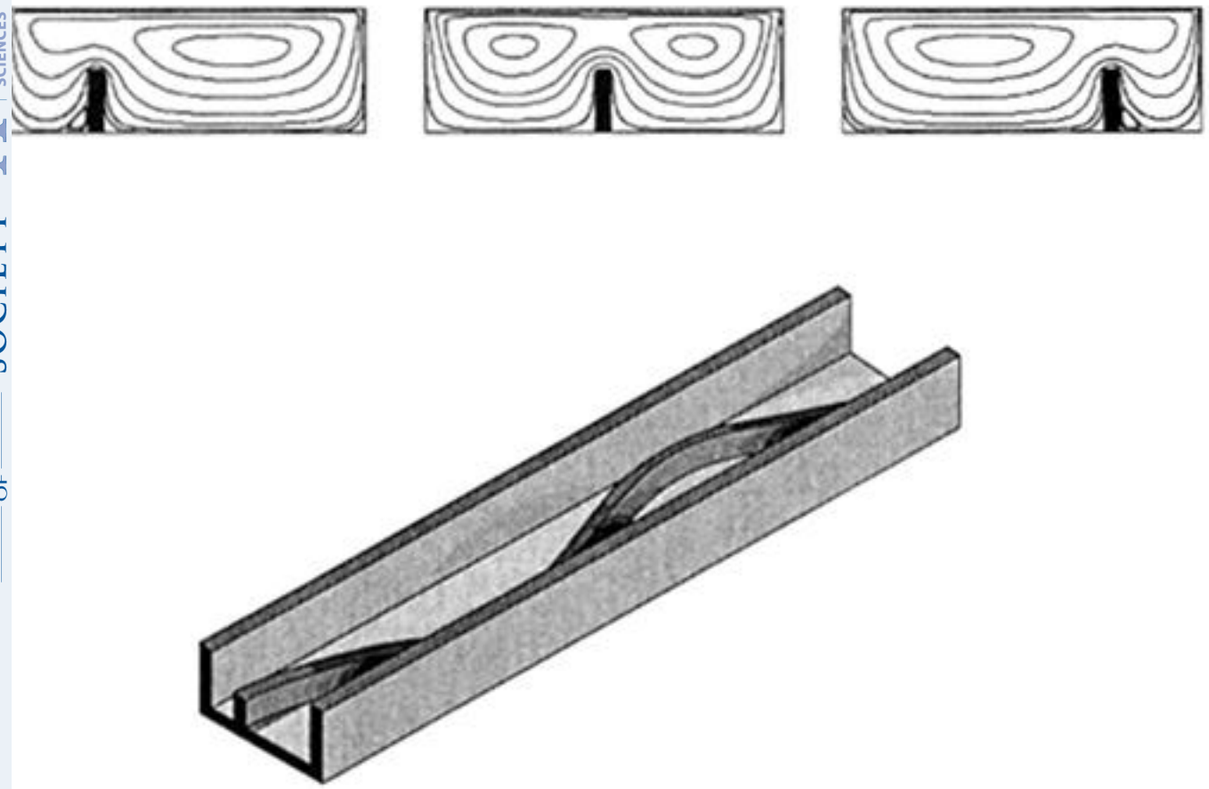

Figure 14

Figure 13. Generation of a time-dependent change in the geometry of a two-dimensional cavity flow by a spatially dependent change in the geometry of the cross section of the corresponding duct flow. Cross-sectional and axial motions are caused by a diagonally moving lid, which is not shown. The top part of the figure computed cross-sectional streamlines corresponding to three different axial locations. Although in the figure the 'snake baffle' is spatially periodic, it could be utilized as an aperiodic recursively generated shape as well.

Figure 14. Mixing in the eggbeater flow achieved utilizing the 'Fibonacci' protocol. All figures utilize $v(\xi)$ even with $V_s = 0$ and $T = 0.4$. The initial state is a line of 50 000 particles placed along $= -0.9$. Compare with figure 6*a*.